Int. J. Electrochem. Sci., 15 **(2020)** 293 – 303, doi: 10.20964/2020.01.11

International Journal of
ELECTROCHEMICAL
SCIENCE
www.electrochemsci.org

The Fabrication of an Impedance Immunosensor Based on Interdigitated Array Microelectrodes and Normalized Impedance Changes for Chlorpyrifos Residue Detection

Wenping Zhao[1,2], Yemin Guo [1,2], Qingxue Zhao[1,2], Jianfei Sun [1,2] , Zhiqiang Wang[2,3], Xia Sun [1,2*]*

[1] School of Agriculture Engineering and Food Science, Shandong University of Technology, No. 12 Zhangzhou Road, Zibo 255049, Shandong Province, P.R. China
[2] Shandong Provincial Engineering Research Center of Vegetable Safety and Quality Traceability, No. 12 Zhangzhou Road, Zibo 255049, Shandong Province, P.R. China
[3] College of Computer Science and Technology, Shandong University of Technology, No. 12 Zhangzhou Road, Zibo 255049, Shandong Province, P.R. China
[*]E-mail: 187286528@qq.com, sunxia2151@sina.com

Received: 21 June 2019 / *Accepted:* 16 October 2019 / *Published:* 30 November 2019

A novel impedance immunosensor was developed based on antibodies fixed on interdigitated array microelectrodes (IDAMs) to detect chlorpyrifos residues. Before use, IDAMs were cleaned using the best method among three methods. Anti-chlorpyrifos monoclonal antibodies were oriented on IDAM surfaces by staphylococcal protein A (SPA). SPA was immobilized on the microelectrode surfaces to provide a better interface for biocompatibility and to increase a fixed amount of antibodies. The immobilized antibodies captured target chlorpyrifos and changed the impedance of the IDAM surface. Electrochemical impedance spectroscopy (EIS) was then used to characterize the change. According to the test results, the best volumes and concentrations of SPA, anti-chlorpyrifos antibodies and BSA drops on IDAMs, as well as the volume and pH of the working buffer used in the experiments were determined. Under the optimal conditions, the correlation between impedance signals and the chlorpyrifos concentration of the incubated electrochemical biosensor was studied. To deal with measured data using normalized impedance and analyze the correlation of two concentrations (1 μg/mL and 10 μg/mL) of chlorpyrifos with impedance signals at seven specific frequencies (1 Hz, 10 Hz, 100 Hz, 1 kHz, 10 kHz, 100 kHz and 1 MHz), the optimal frequency (100 Hz) was selected. The standard curve was drawn after extracting the impedance values under different concentrations of pesticides at the frequency of 100 Hz. To determine the normalized impedance change (NIC) at 100 Hz against the logarithm from 1 ng/mL to 100 μg/mL of the chlorpyrifos concentration (LgC), the used regression equation was y = 132.62x + 733.1, with a linear correlation coefficient of 0.9946. The lowest limit of detection (LOD) for this biosensor was 1 ng/mL. The immunosensor showed good specificity and sensitivity for chlorpyrifos detection.

Keywords: Immunosensor; Chlorpyrifos; Interdigitated array microelectrode; Normalization

1. INTRODUCTION

The high toxicity of organophosphorous (OP) pesticides and their cumulative effects in animals cause a great impact on human health [1-3]. Chlorpyrifos (CP) is a type of OP pesticide widely used against agricultural pests to enhance crop production and has been reported as the second most common pesticide detected in food and water [4-5].

Therefore, rapid and sensitive determination of CP pesticides has become increasingly important for human health protection. In recent years, electrochemical impedance sensors have attracted a great deal of interest in antibody-antigen-based sensors [6-8] because they are a more sensitive approach when compared with conventional amperometric biosensors, which heavily rely on the relative closeness between active sites and electrode surfaces in obtaining signals [9].

Electrochemical impedance spectroscopy (EIS) is often used as a sensitive technique for analysis of interfacial properties related to bio-recognition events, such as enzyme-catalyzed reaction and biomolecular recognition events of specific binding proteins, antibodies or antibody-related substances occurring at the modified surface [10].

Most researches on impedimetric biosensors are associated with immune sensors and aptasensors [11-13]. In these biosensors, antigens bind to antibodies to form immunocomplexes, which attach to electrode surfaces, increasing the resistance of electron transport so as to inhibit electron transfer. Impedimetric biosensors are an enzyme-label-free means for detecting biomolecular recognition signals.

In order to achieve a lower limit of detection (LOD) while using fewer immunosensors, a better choice is to use microelectrodes, rather than macroelectrodes, in parallel with conventional test methods. In comparison with macroelectrodes, for which reactants are more easily depleted, microelectrodes allow for a more sustainable supply of reactants. Microelectrodes require a lower concentration of electroactive ions than macroelectrodes for the purpose of producing double layers [14-17]. To sum up, microelectrodes help conduct impedance measurement even in a low conductivity solution, whereas macroelectrodes may not be sensitive in this situation.

Interdigitated array microelectrodes (IDAMs) have many promising benefits for electrochemical tests. For instance, IDAMs could establish a new steady-state condition to shorten the detection time and require a low ohmic drop to maximize impedance changes on electrode surfaces, reducing the interference to other analytes in the test solution and improving the signal-to-noise ratio (SNR) [18-20]. However, IDAMs are expensive and not easy to be fabricated, which require careful cleaning for reuse due to the sags and crests on their surfaces.

In our research, a novel method for sensitive chlorpyrifos residue detection based on IDAMs was proposed. The immunosensor was built using SPA from staphylococcus aureus. Anti-chlorpyrifos monoclonal antibodies were immobilized on the SPA and then used to modify microelectrodes. Chlorpyrifos residues of different concentrations would be arrested by the antibodies, leading to impedance changes on the IDAM surfaces. The changes were depicted by means of EIS. The normalized impedance change (NIC) was required for processing the measured data at the optimal frequency (100 Hz), which was then used to analyze the correlation between the logarithm of chlorpyrifos concentrations (LgC) and the NIC data under specific frequencies. The regression formula for the NIC against the logarithm of the chlorpyrifos concentration from 1 ng/mL to 100 μg/mL could be obtained. It provided theoretical support for subsequent biosensor preparation and pesticide detection.

2. EXPERIMENTAL AND METHODS

2.1 Reagents and materials

Protein A, bovine serum albumin (BSA), anti-chlorpyrifos monoclonal antibodies and chlorpyrifos were all obtained from Sigma-Aldrich (St. Louis, MO, USA). To dissolve anti-chlorpyrifos monoclonal antibodies, phosphate buffered saline (PBS, 10 mM, pH 7.2-7.4) was used as a solution for chlorpyrifos detection, which included 0.1 M KCL and 5 mM $[Fe(CN)_6]^{3-/4-}$. Reconstitution of BSA and SPA was performed using PBS. The blocking solution was also prepared based on BSA using PBS (1.0%, w/v). Deionized water was prepared in a Milli-Q system (Millipore, 18.2 MΩ•cm), which was then used to produce other required solutions. Furthermore, the other reagents were of analytic grade or higher.

2.2 Apparatus and impedance measurement

Gold IDAMs (IME AU-1550.5) were bought from ABtech Scientific Inc. (Richmond, VA, USA), each of which possessed 50 digital pairs with a digit length of 4985 μm, a digital width of 15 μm and an interdigital space of 15 μm. The total area for the electrodes was 14.88 mm^2. Figure 1A shows an IDAM.

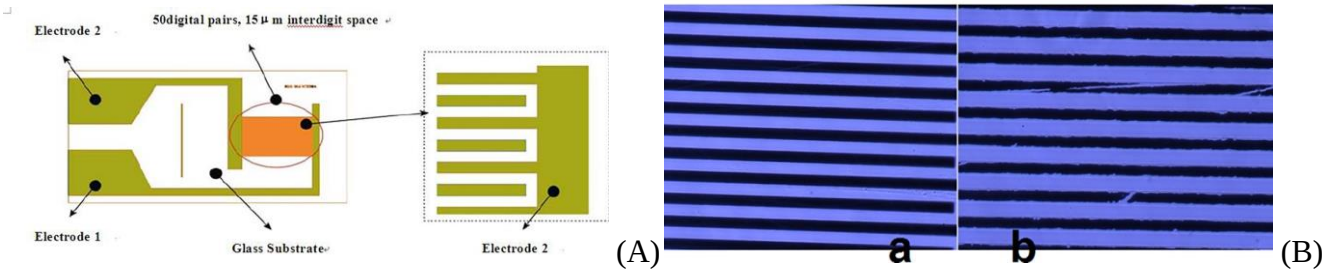

Figure 1. Interdigitated array microelectrode

Compared with conventional electrodes, IDAMs have a higher mass transfer rate, smaller double-layer charging current (Ic) and lower time constant (R_C) [21, 22].

Impedance measurements were performed using an IM-6 impedance analyzer (BAS, West Lafayette, IN, USA) with IM-6/THALES software. One pole of the IDAM was connected to both the test and sense probes and the other pole was connected to both the reference and counter electrodes of the IM-6 impedance analyzer. All impedance measurements were conducted in the presence of 5 mM $[Fe(CN)_6]^{3-/4-}$ (1:1) and 0.1 M KCL mixture in 0.1 M PBS (pH 7.4), which were used as a redox probe. The tested frequency range from 1 Hz to 1 MHz with an amplitude of 5 mV was selected, and Bode (impedance and phase vs frequency) and Nyquist (imaginary impedance vs real impedance) diagrams were recorded.

2.3 Biosensor fabrication and pesticide detection

The entire experiment involves electrode cleaning, SPA immobilization, antibody fixation, BSA blocking and pesticide antigen detection.

2.3.1 Electrode cleaning

Three cleaning methods were used to deal with a bare electrode, and the best method was selected. In method 1 (M1), IDAMs were cleaned using acetone (CH_3COCH_3), alcohol (C_2H_5OH) and deionized water, and then dried using nitrogen [23]. In method 2 (M2), IDAMs were cleaned by 0.1 M sodium hydroxide (NaOH) for 15 min, 0.1 M hydrochloric acid (HCl) for 15 min, acetone for 5 min and deionized water, and then dried by nitrogen [24]. In method 3 (M3), according to the reference literature [25] with slight modification, IDAMs were immersed in 1 M NaOH for 15 min, washed by deionized water, immersed in 1 M HCl for 15 min, washed by deionized water, and then gently cleaned with lens paper containing alcohol for 5 min. After the final wash, the electrodes were dried with a stream of nitrogen. Then, the IDAMs were ready for surface modification and antibody immobilization.

Subsequently, the microelectrodes were observed using a microscope (40 x 40) to seek for unknown features, spoiled microelectrodes or abnormal objects (Fig. 1B-b). If unknown features were not found (Fig. 1B-a), impedance could be measured for the microelectrodes with 5 mM $[Fe(CN)_6]^{3-/4-}$ (1:1) and 0.1 M KCL mixture in 0.1 M PBS (pH 7.4). This impedance value was compared with the previous one measured for bare electrodes. New antibodies could be applied on the microelectrodes if the values were similar, or another cleaning step would be performed if the values were different.

Note that the microelectrodes could be reused after a cleaning procedure as above.

2.3.2 Electrode surface immobilization and fixation

The cleaned IDAMs were incubated for 50 min with 30 μL of SPA solution (10 μg/mL) under 22-25°C. Subsequently, they were washed to eliminate non-combined SPA by deionized water, dried by streams of nitrogen and then incubated for 1 h at 4°C with 30 μL antibodies (100 μg/mL). After that, the IDAMs were incubated for another 1 h with 30 μL of 5% BSA under 4°C. Following another round of rinsing and drying, the IDAMs were prepared to be ready for detection. Scheme 1 illustrates the immunosensor preparation process.

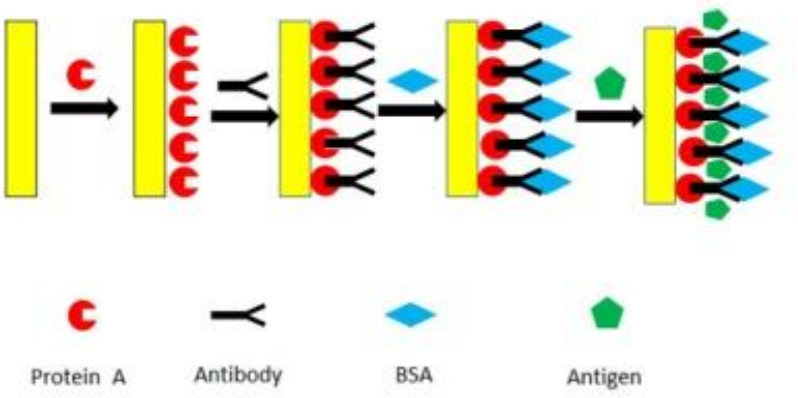

Scheme 1. The process of assembling electrochemical immune sensors

3. RESULTS AND DISCUSSION

3.1 Determination of the best IDAM electrode cleaning method

By measuring the Faradaic impedance with a redox probe like $[Fe(CN)_6]^{3-/4-}$ [26, 27], the impedance biosensor obtained its basic transduction characteristics. As biolayers formed on electrode surfaces, $[Fe(CN)_6]^{3-/4-}$ no longer performed electron transfer, increasing resistance to electron transfer. To detect surface-altered electrode features, a significantly effective approach was to use EIS [28].

Since the IDAM surface was full of sags and crests and the gold layer was so thin that it was not easy to clean but prone to damage. This experiment optimized the cleaning methods not to damage the electrode structure while retaining the best cleaning effect. Three different cleaning programs (mentioned in 2.3.1) were implemented to investigate the cleaning effects by comparing the impedance with each other (Fig. 2 and 3).

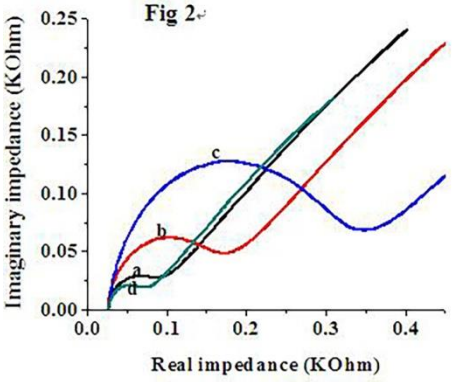

Figure 2. The electrode impedance spectroscopy using different cleaning methods. (a) Bare IDAM; (b) SPA/IDAM; (c) SPA/IDAM cleaned by M1; (d) SPA/IDAM cleaned by M2.

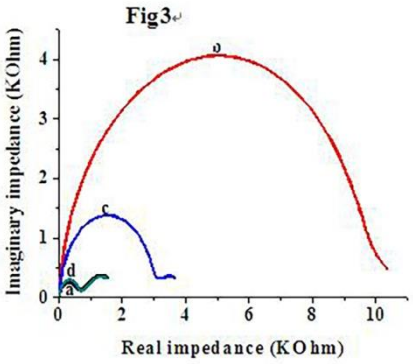

Figure 3. The electrode impedance spectroscopy using different cleaning methods. (a) Bare IDAM; (b) BSA/antibody/SPA/IDAM; (c) BSA/antibody/SPA/IDAM cleaned by M2; (d) BSA/antibody/SPA/IDAM cleaned by M3.

Fig. 2 shows the impedance obtained from a bare IDAM (curve a), SPA/IDAM (curve b), SPA/IDAM cleaned by M1 (curve c) and SPA/IDAM cleaned by M2 (curve d) by applying the $[Fe(CN)_6]^{3-/4-}$ probe. Fig. 3 shows the impedance obtained based on a redox probe $[Fe(CN)_6]^{3-/4-}$ from a bare IDAM (curve a), BSA/antibody/SPA/IDAM (curve b), BSA/antibody/SPA/IDAM cleaned by M2 (curve c) and BSA/antibody/SPA/IDAM electrode cleaned by M3 (curve d).

Excessive low resistance existed on the surface of a bare IDAM (curve a of Fig. 2 and 3). When the electrode surface was applied with SPA (curve b of Fig. 2), or with SPA, antibody and BSA (curve b of Fig. 3), the resistance was greatly higher than that measured for a bare IDAM. That was because SPA, antibody and BSA were macromolecules possessing bioactive but no conductive characteristics. The resistance increase of the SPA/IDAM surface was due to direct adsorption of SPA, which was according to Van der Waals force. Then, anti-chlorpyrifos monoclonal antibodies were fixed on the surface of the sensor because of the affinity of SPA to antibodies' F_c [29, 30]. In this case, the F_{ab} binding sites of the antibodies were directed away from the SPA-changed solid support, so that immobilization of these antibodies achieved excellent immune reaction. Consequently, the blocking solution of BSA was used for the purpose of inhibiting non-target surface sites and reducing adsorption of non-targets.

When M1 (curve c of Fig. 2) and M2 (curve d of Fig. 2) were used to deal with the SPA/IDAM, the results showed that M2 was better than M1. Curve c and curve d in Fig. 2 indicated that M2 could remove SPA from the electrode but M1 could not. Similarly, when M2 (curve c of Fig. 3) and M3 (curve d of Fig. 3) were used to deal with the SPA/IDAM, the results indicated that M3 was better than M2. Curve c and curve d in Fig. 3 demonstrated that M3 could remove SPA from the electrode while M2 could not.

In brief, the best IDAM cleaning method was M3, which was described in 2.3.1.

3.2 Determination of the best concentration and amount of SPA

SPA served as the interface between IDAMs and antibodies immobilized on the IDAM surfaces, and its concentration and dropping amount had an influence on the quantity of the modified antibodies. If the concentration was too low, the electrode surface would be incompletely modified, and the gold IDAM would directly contact with the antibody so that the gold layer would affect the antibody activity. If the concentration of SPA was too high, excess SPA would make itself easy to fall from the IDAM surface, and some antibodies in contact with SPA would fall off from the surface, resulting in constant or reduced electron transfer resistance in EIS. Therefore, this experiment optimized the concentration and quantity of SPA.

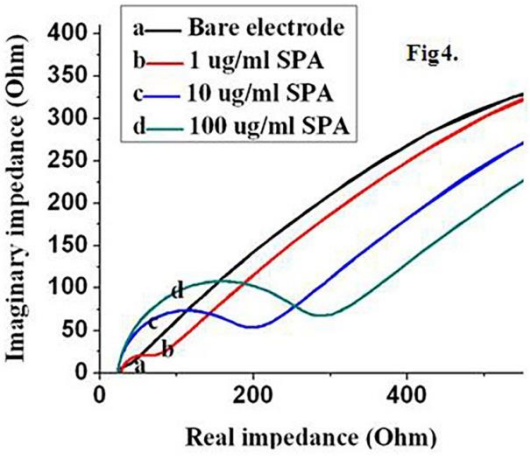

Figure 4. Impedance spectroscopy of IDAMs modified with different concentrations of SPA. (a) Bare IDAM; (b) 1 μg/mL SPA/IDAM; (c) 10 μg/mL SPA/IDAM; (d) 100 μg/mL SPA/IDAM.

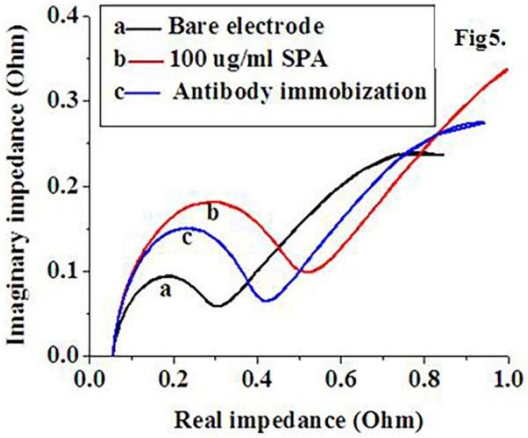

Figure 5. Impedance spectroscopy of IDAMs modified with 100 μg/mL SPA and 100 μg/mL antibody. (a) Bare IDAM; (b) SPA/IDAM; (c) Antibody/SPA/IDAM.

According to the reference [23], the concentration of SPA was 100 μg/mL. This experiment adopted three gradient concentrations of SPA (1, 10 and 100 μg/mL). According to the IDAM area, 30 μL of SPA could completely cover the electrode, and therefore 30 μL was the optimum amount.

Fig. 4 showed the EIS results obtained from a bare IDAM (curve a), 1 μg/mL SPA/IDAM (curve b), 10 μg/mL SPA/IDAM (curve c) and 100 μg/mL SPA/IDAM (curve d) using the redox probe $[Fe(CN)_6]^{3-/4-}$. Fig. 5 showed the EIS results obtained from a bare IDAM (curve a), 100 μg/mL SPA/IDAM (curve b) and antibody/SPA/IDAM (curve c) using $[Fe(CN)_6]^{3-/4-}$. Fig. 4 revealed that the impedance increased remarkably (curves a, b, c and d) with the increasing concentration of SPA. In

contrast, Fig. 5 showed that too much SPA (100 μg/mL) made it fall off from the electrode easily. Some of the antibodies in contact with SPA fell off from the electrode surface and even caused unmodified antibodies, leading to constant or reduced electron transfer resistance in EIS. The best concentration of SPA chosen in this experiment was therefore 10 μg/mL.

3.3 Determination of the optimal frequency in impedance spectroscopy for chlorpyrifos detection

BSA/antibody/SPA/IDAMs without chlorpyrifos were all utilized in this study as the control. To check the influence of impedance measurement on different types of pesticides, the magnitude of impedance with and without chlorpyrifos was compared. The normalized impedance change (NIC) values were given in following formula:

$$\mathrm{NIC} = \frac{Z_{\mathrm{sample}} - Z_{\mathrm{control}}}{Z_{\mathrm{control}}} \times 100 \quad (1)$$

In this formula, $Z_{control}$ and Z_{sample} represent the degree of impedance for the control and chlorpyrifos samples, respectively.

The frequencies for the EIS tests ranged from 1 Hz to 1 MHz. In actual applications, 1 Hz, 10 Hz, 100 Hz, 1 kHz, 10 kHz and 100 kHz were chosen.

The impedance values of seven frequencies with or without chlorpyrifos at the two concentrations were used to calculate the electrode impedance changes before and after incubation and NIC, and the results were shown in Table 1, where ID stands for impedance difference.

The difference was indicated by the NIC, as illustrated in Table 1. The value increased from 19.43% (1 μg/mL) and 50.53% (10 μg/mL) to 26.08% and 79.76% when the frequency changed from 1 Hz to 100 Hz. Then, the values decreased from 26.08% (1 μg/mL) and 79.76% (10 μg/mL) to 1.54% and 2.02% when the frequency changed from 100 Hz to 1 MHz. Therefore, the best frequency was chosen as 100 Hz.

Table 1. Impedance differences at different frequencies and the NIC values

Frequency (Hz)	1 μg/mL (ID/Ω)	10 μg/mL (ID/Ω)	1 μg/mL (NIC/%)	10 μg/mL (NIC/%)
1	1384.6	1153	19.43	50.53
10	1346.1	1152.7	24.21	68.23
100	1249.3	1130	**26.08**	**79.76**
1 k	587.2	600.3	16.33	51.68
10 k	12.05	16.74	1.54	5.6
100 k	1.89	1.338	1.72	3.19
1 M	1.625	0.538	3.61	2.02

3.4 Impedance measurement and extraction of the regression equation

According to Fig. 6, the regression equation was y = 132.62x + 733.1 with R^2 = 0.9946, indicating the linearity between the NIC values at 100 Hz and the logarithm of the chlorpyrifos concentration (LgC, LgC = x) ranging from 1 ng/mL to 100 μg/mL. The lowest LOD for this biosensor was 1 ng/mL.

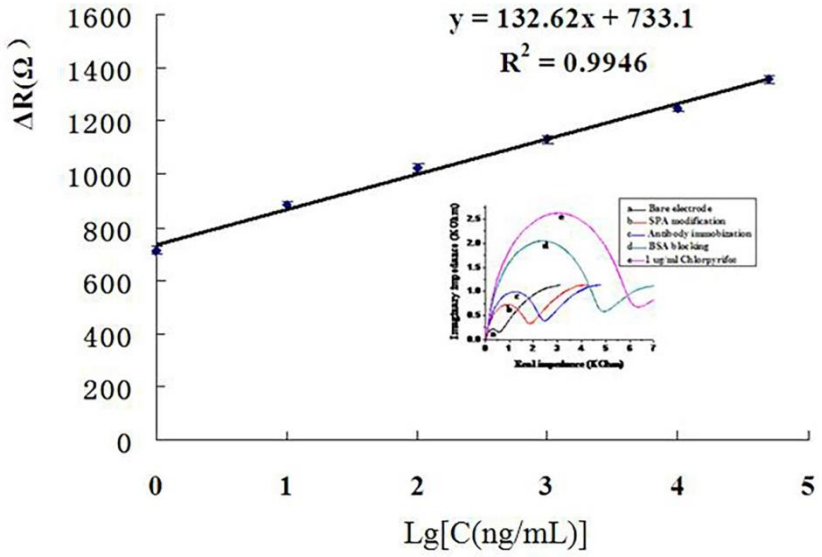

Figure 6. The regression equation between the chlorpyrifos concentration and the impedance on the electrode

Table 2 showed the performance of the BSA/anti-chlorpyrifos/SPA/IDAM sensor compared with other reported immunosensors for the detection of chlorpyrifos in recent years. As shown in Table 2, compared with other methods, the immunosensor developed in this study had a relative large linear range and lower detection limit, indicating that the proposed sensor is reliable for the determination of chlorpyrifos pesticides. More importantly, the preparation process of this sensor was simple, the use of the IDAM electrodes reduced the consumption of biochemical reagents, and the application of the normalized impedance method provided possibility of using portable signal detection devices connected to them.

Table 2. Comparison of the sensor with other similar immunosensors for chlorpyrifos detection

Working Electrode	Modified Material	Linear Range and LOD	Detection Technique	References
GCE	AChE/PAMAN-Au/CNTs	4.8×10^{-9} M - 0.9×10^{-7} M; 4.0×10^{-9} M	CV	[31]
GCE	MWCNTs-THI-CHIT	0.1-1.0×10^{5} ng/mL; 0.046 ng/mL	CV, DPV and EIS	[32]

GCE	AChE/CPBA/GR-AuNPs	0.5-10 ng/mL, 10-100 ng/mL, and 0.1 ng/mL	CV and EIS	[33]
FTO	AuNPs-chlAb	10 fM, 1 fM to 1 μM	CV and DPV	[34]
SPE	AChE/MWCNTs-TCNQ	0.35-35 ng/mL, 0.1 ng/mL	CV IT EIS	[35]
GCE	AChE-CdS-G-CHIT	2 ng/mL - 2 g/mL; 0.7 ng/mL	CV and EIS	[36]
IDAM	SPA	1 ng/mL - 100 μg/mL; 1 ng/mL	EIS	our work

4. CONCLUSION

In this work, an innovative impedance biosensor was developed for direct measurement of impedance aiming for chlorpyrifos detection. This biosensor was based on antibodies immobilized on new IDAM surfaces with the help of SPA modification. IDAMs were cleaned with different methods, and the best cleaning method was selected to adapt to the thin gold layer of the IDAM electrode. Polyclonal antibodies against chlorpyrifos were directed to the surface based on SPA. Following antibody fixation, BSA was employed to block non-specific binding sites. The best volumes and concentrations of SPA (30 μL and 10 μg/mL), anti-chlorpyrifos antibody (30 μL and 100 μg/mL) and BSA drops (30 μL and 5 mg/mL) on IDAMs, and the volume and pH of the working buffer (50 μL and 7.5) were determined. Using the normalized impedance method to deal with the measured data and analyze the correlation between two different concentrations of chlorpyrifos at seven specific frequencies (1 Hz, 10 Hz, 100 Hz, 1 kHz, 10 kHz, 100 kHz and 1 MHz) and impedance signals, the optimal frequency (100 Hz) was selected. It provided theoretical support for subsequent preparation of biosensors and detection of pesticides.

However, in our work, there were only three concentration gradients of SPA selected to modify the electrodes and two concentrations of chlorpyrifos selected to incubate the electrodes. In our future research, more concentration gradients would be added.

ACKNOWLEDGMENTS

This work was supported by the National Natural Science Foundation of China (No. 31772068, 31701681 and 31872909), Special Project of Independent Innovation of Shandong Province (2018CXGC0214), Shandong Provincial Natural Science Foundation (ZR2019MC063, ZR2018ZC0126, ZR2018BC055, and ZR2017BC001), Key Research and Invention Program of Shandong Province (2017GNC10119), Key Innovative Project for 2017 Major Agriculture Application Technology of Shandong Province, School and City Integration Development Project of Zibo (2018ZBXC342 and 2018ZBXC323).

Refernces

1. Y. Liu, D. Shen, R. Mo and F. Tang, *J. Food Sci.,* 78(2) (2013) 372-376.
2. M. Balali-Mood, K. Balali-Mood, M. Moodi and B. Balali-Mood, *Iranian Journal of Public Health,* 41(10) (2012) 1-14.
3. M. Sánchez-Guerra, N. Pérez-Herrera and B. Quintanilla-Vega, *Toxicol. Mech. Methods,* 21(9)

(2011) 681-691.
4. M.D. Cupic, S. Borozan and S. Ivanovic, *Poult. Sci.,* 97(5) (2018) 1564-1571.
5. E.M. John and J.M. Shaike, *Environ. Chem. Lett.,* 13(3) (2015) 269-291.
6. J. Dong, H. Zhao, M. Xu, Q. Ma and S. Ai, *Food Chem.,* 141(3) (2013) 1980-1986.
7. G. Liu, J. Liu, T.P. Davis and J.J. Gooding, *Biosens. Bioelectron.,* 26(8) (2011) 3660-3665.
8. R. Elshafey, A.C. Tavares, M. Siaj and M. Zourob, *Biosens. Bioelectron.,* 50(4) (2013) 143-149.
9. J. Wang, J.A. Profitt, M.J. Pugia and I.I. Suni, *Anal. Chem.,* 78 (2006) 1769.
10. E.B. Bahadır and M.K. Sezgintürk, *Artificial Cells,* 44(1) (2014) 1-15.
11. U. Jarocka, H. Radecka, T. Malinowski, L. Michalczuk, & J. Radecki, 25(2) (2013)433-438. 12.
12. E.B. Aydın and M.K. Sezgintürk, An impedimetric immunosensor for highly sensitive detection of il-8 in human serum and saliva samples: a new surface modification method by 6-phosphonohexanoic acid for biosensing applications. *Anal. Biochem.,* 185 (2018) 44-52.
13. L. Madianos, G. Tsekenis, E. Skotadis, L. Patsiouras and D. Tsoukalas, *Biosens. Bioelectron.,* 101 (2018) 268.
14. M. Ciszkowska and Z. Stojek, *J. Electroanal. Chem.,* 466 (1999)129.
15. M. Marrakchi1, I. Campos Sánchez, S. Helali, N. Mejri, J. Soto Camino, M. A. Gonzalez-Martinez, M. Hamdi, A. Abdelghani. Sensor Letters, 9(6) 2011,2203-2206.
16. H. Wang, X. Wu, P. Dong, J. Wang, D. Di and C. Jian, *Micro & Nano Letters,* 8(1) (2013) 11-14.
17. A. Bajwa, S. Tan, R. Mehta and B. Bahreyni, *Sensors,* 13(7) (2013) 8188-8198.
18. M. Čerňanská, P. Tomčík, Z. Jánošíková, M. Rievaj and D. Bustin, *Talanta,* 83(5) (2011) 1472-1475
19. X. Tang, D. Flandre, J.P. Raskin, Y. Nizet, L. Moreno-Hagelsieb, R. Pampin and L.A. Francis, *Sens. Actuators, B: Chemical,* 156(2) (2011) 578–587
20. X. Yan, M. Wang and D. An, *Chin. J. Anal. Chem.*, 39(10) (2011) 1601–1610
21. K.V. Singh, A.M. Whited, Y. Ragineni, T.W. Barrett, J. King and R. Solanki, *Anal. Bioanal. Chem.,* 397(4) (2010) 1493-1502.
22. M. Marrakchi, I.C. Sánchez, S. Helali, N. Mejri, J.S. Camino and M.A. *Sensor Letters,* 9(6) (2011) 2203-2206.
23. X. Jiang, R. Wang, Z. Ye, J. Wang, Y.Li and Y. Ying, *An ASABE Meeting Presentation*, (2008)
24. M. Varshney and Y. Li, *Biosens. Bioelectron.,* 22 (2007) 2408.
25. R. Wang, Y. Wang, K. Lassiter, Y. Li, B. Hargis, S. Tung, L. Berghmand and W. Bottje, *Talanta,* 79 (2009) 159.
26. J. Cecchetto, F.C. Carvalho, A. Santos, F.C.B. Fernandes and P.R. Bueno, *Sens. Actuators, B: Chemical,* 213 (2015) 150-154.
27. X. Xiong, X. Shi, Y. Liu, L. Lu and J. You, 10(2018) 365-370
28. L. Fan, G. Zhao, H. Shi, M. Liu and Z. Li, *Biosens. Bioelectron.,* 43(1) (2013) 12-18.
29. T. Champion and A. Beck, *Methods Mol. Biol.,* 988 (2013) 331-343.
30. G. Fassina, A. Verdoliva, M.R. Odierna, M. Ruvo and G. Cassini, *J. Mol. Recognit.,* 9(5-6) (1996) 564-569.